Environmental Science Nano

Accepted Manuscript

ROYAL SOCIETY OF CHEMISTRY

rsc.li/es-nano

Cite this: DOI: 10.1039/c0xx00000x

www.rsc.org/xxxxxx

ARTICLE TYPE

Salinity increases the toxicity of silver nanocolloids to Japanese medaka embryos

Chisato Kataoka,[ab] Tadashi Ariyoshi,[a] Hideo Kawaguchi,[a] Seiji Nagasaka[ab] and Shosaku Kashiwada[ab]*

Received (in XXX, XXX) Xth XXXXXXXXX 20XX, Accepted Xth XXXXXXXXX 20XX

DOI: 10.1039/b000000x

To investigate the effects of salinity on the toxicity of silver nanocolloids (SNCs, 28.4 nm in diameter) in aquatic environments (freshwater, brackish water, and seawater), we exposed 15 medaka eggs in triplicate to SNCs at 10 mg/L in different salinities of embryo-rearing medium (ERM) (1×, 5×, 10×, 15×, 20×, and 30×) until hatching (1× ERM and 30× ERM have osmotic pressures equivalent to freshwater and seawater, respectively). With increasing concentration of ERM, SNCs aggregated to 437.3 nm in diameter in 30× ERM solution. Simultaneously, soluble silver chloro complexes (various combinations of $[AgCl]^0$, $[AgCl_2]^{1-}$, $[AgCl_3]^{2-}$, and $[AgCl_4]^{3-}$) were calculated to have been formed. The patterns of the absorption spectra of SNCs and $AgNO_3$ (a reference compound) differed markedly in ERM at different salinities, indicating that different soluble silver complexes were present in each solution. With increasing salinity, the chorion resistance decreased, and the salinity in the medaka eggs, as indicated by the osmotic pressure, increased. Simultaneously, uptake of SNCs or other silver complexes into the embryos also increased compared with that of $AgNO_3$ in 20× and 30× ERM. In the presence of SNCs in 20× ERM, embryo hatching rate and full body lengths of post-hatch larvae were significantly lower than with $AgNO_3$. The toxic effects of SNCs on hatching rate increased significantly in media of high salinity and were greater than those of $AgNO_3$. SNCs and related silver chloro complexes exhibited higher bioavailability and medaka embryo toxicity in saline conditions than did $AgNO_3$. SNCs pose greater ecological risks to fish embryos in high-salinity aquatic environments than in freshwater environments.

Nano impact

Little information is available on the environmental fate of nanomaterials, including silver nanocolloids (SNCs). Environmental factors such as salinity, pH, and temperature could influence the fate of such materials. Salinity—one of the most important aquatic environmental factors—is likely to affect the fate of SNCs, including soluble silvers such as silver chloro complexes. We demonstrated that the bioavailability of SNCs and related soluble silver compounds was greater in seawater than in freshwater, thus increasing the toxicity of SNCs to medaka embryos compared with that of a control $AgNO_3$ solution. Our findings provide novel insights into the aquatic environmental interactions and ecological risks of silver nanomaterials in terms of environmental health.

Introduction

Numerous chemicals are being developed to improve and maintain human quality of life, but the release of such chemicals and chemical wastes into the environment can pose ecological risks. Because nanomaterials and nano-industries are emerging rapidly on international markets,[1] the ecological risks posed by nanomaterials must be considered. Silver nanomaterials have been developed mainly as antibacterial healthcare products and now account for half of the international nanomaterial market.[2] Along with this rise in use of silver nanomaterials have come studies of their toxicity. For example, the toxicity of silver nanoparticles to zebrafish (*Danio rerio*) embryos is dose dependent in terms of increased mortality, decreased heart rate, reduced hatching rate, abnormal development, and increased catalase activity; mortality is also particle-size dependent[3–5] and capping-material dependent.[3] Silver ions released from silver nanomaterials are considered to be important factors in the toxicity of silver nanomaterials; the release efficiency of silver ions depends on the type or presence of capping material.[6] To minimise the toxic effects of capping materials, and to study the toxic effects of nano-sized silver, water-dispersed nanocolloidal silver with uncapped and naked particles has been employed.[7] Previously, using Japanese medaka (*Oryzias latipes*), our research team revealed that the abnormalities in embryo development induced by silver nanocolloids (SNCs) were attributable to the disruption of embryogenesis gene expression.[7] However, there is little information on the mechanism of toxicity of silver nanomaterials or on their ecological effects.

To address the ecological issue of silver nanomaterials, bioassays have been performed in fish, algae, daphnia, sea urchins, shrimp, sea hares, and coral.[3,8–12] Fish eggs and post-hatch larvae are more susceptible than the adult stage to chemical exposure. The chemical susceptibility of these fish stages is advantageous in aquatic toxicological studies, as it helps us to

understand and predict the ecological risks of chemicals. Fish eggs have a chorion that protects the embryo from the surrounding environment;[13] the mechanism by which xenobiotics permeate through the chorion remains unclear. Mucus is likely to play a role in the cell membrane permeation and bioavailability of nanoparticles.[14,15] Hayashi *et al.*[16] have found in earthworms that wrapping the nanoparticles in a native protein corona helps in cellular interaction and membrane permeation of the nanoparticles. Fish gills, which are covered in mucous membrane, play the most important role in the uptake of xenobiotics in larvae and adult fish. Fish gills are among the target organs in nanotoxicology,[17] and Yue *et al.*[18] have reported the toxicity of silver nanoparticles to a fish gill cell line. However, in medaka embryogenesis the gills are still not functional at stage 31 (3 days before hatching),[19] which means that the gills are not yet a route of uptake of silver nanoparticles. The chorion has no mucus and has soft tissue on its surface. Sakaizumi[20] studied the toxic interactions between methyl mercury and salinity in Japanese medaka eggs and found that increasing the osmotic pressure of the test solution enhanced the toxicity of the methyl mercury. Sumitani *et al.*[21] used medaka eggs to investigate the toxicity of landfill leachate; they found that osmotic equivalency of leachate to eggs was the key to inducing abnormalities in embryogenesis. Furthermore, in our previous study[22] we found that plastic nanoparticles (39.4 nm in diameter) easily permeated the medaka egg chorion under brackish conditions [500 mOsm in 15× embryo-rearing medium (ERM)].

It was initially considered possible that, in Pleuronectidae fishes, chemicals could permeate through the egg chorion *via* pores distributed on its surface; however, scanning electron microscope (SEM) images have revealed that these pores do not go right through the chorion.[23] We therefore still do not know how nanoparticles penetrate the fish egg chorion. However, the studies mentioned above have shown that chemical bioavailability in the egg is affected by the ambient osmotic pressure.

Japanese medaka is commonly used as a typical freshwater fish model in toxicology[24] and ecotoxicology.[25] Thirteen *Oryzias* species have been identified in East to South Asia, and most of these inhabit marine or brackish waters.[26] Although Japanese medaka is a freshwater fish, it is able to live in not only freshwater but also brackish water or seawater. Because Japanese medaka has evolved in moving northward from south Asia, it has adapted to high-salinity conditions and has highly developed chloride cells.[27] Hence, Japanese medaka eggs are able to hatch normally in seawater (within 8 to 10 days at 25 ºC).[28] These characteristics make this species markedly different from other freshwater fish models such as the zebrafish. Our goal here was to use Japanese medaka embryos to evaluate the effects of environmental aquatic salinity on the bioavailability and toxicity of nano-sized silver.

Materials and methods

Silver nanocolloids

Purified SNCs (20 mg/L, 99.99% purity, 81.1% Ag^+ at pH 7, mean particle diameter *ca*. 28.4 ± 8.5 nm suspended in distilled water; see SEM image in Fig. S1) were purchased from Utopia Silver Supplements (Utopia, TX, USA). Diluted SNC solution (a mixture of silver colloids and Ag^+) for exposure tests was prepared with different concentrations of ERM (1×, 5×, 10×, 15×, 20× or 30×) (1× ERM consisted of 1.0 g NaCl, 0.03 g KCl, 0.04 g $CaCl_2 \cdot 2H_2O$ and 0.163 g $MgSO_4 \cdot 7H_2O$ in 1 L of ultrapure water; pH adjusted to 7.2 with 1.25% $NaHCO_3$ in ultrapure water) to simulate conditions ranging from freshwater to seawater. $AgNO_3$ was used as a reference compound for SNCs. See Supplemental Information for details.

Medaka eggs

Eggs of *O. latipes* orange-red strain at embryonic developmental stage 21 (brain regionalisation and otic vesicle formation stage) were harvested, rinsed with 1× ERM, and then used in the exposure tests. All medaka embryos used were at stage 21, because our previous study had revealed that this stage was more sensitive than other stages to SNCs.[7] See Supplemental Information for details.

Toxicity testing of SNCs at 1× ERM (freshwater conditions)

To examine the toxic effects of SNCs on medaka embryos, 15 medaka eggs (stage 21) in triplicate were exposed to 5 mL of SNCs (1, 5, 10 or 18 mg/L) in 1× ERM at pH 7 during incubation at 25 ºC in the dark until hatching or for 14 days. The test solutions were renewed once a day. During exposure, every day, exposed eggs were observed under a dissecting microscope (SZ-ET, Olympus Co., Tokyo, Japan). The cumulative hatching rate was counted for 14 days. Medaka eggs in 1× ERM at pH 7 without SNCs were used as controls. To examine the effects of the ERM on SNC toxicity, we replaced the ERM with ultrapure water at pH 7. Full details of the method used are given in our previous paper.[7] See Supplemental Information for details.

Wave scanning of silver solutions

For qualitative analysis of SNCs or $AgNO_3$, or of silver soluble chloro complex formation ($[AgCl]^0$, $[AgCl_2]^-$, $[AgCl_3]^{2-}$ and $[AgCl_4]^{3-}$), the absorbances of 10 mg/L of SNC or $AgNO_3$ solution (in 1×, 5×, 10×, 15×, 20×, or 30× ERM, or in ultrapure water) and of 0.625, 1.25, 2.5, 5, and 10 mg/L of SNC or $AgNO_3$ solution in 30× ERM were scanned in triplicate with a UV-Vis-NIR spectrophotometer (UV-3600, Shimadzu Co., Kyoto, Japan). SNC or $AgNO_3$ solution was mixed with each ERM or with ultrapure water. The mixture was left at room temperature for 24 h and then subjected to scanning. Portions of the SNC solutions were filtered through a 3-kDa membrane filter to examine the absorbance of soluble silvers without particles. Both filtered and unfiltered solutions were subjected to scanning. See Supplemental Information for details.

Salinity-dependent production of silver chloro complexes

Formation of silver chloro complexes was calculated by using the free program Visual MINTEQ version 3.0 (http://www.lwr.kth.se/English/OurSoftware/vminteq); we also used stepwise formation constants for Cl^- and Ag^+.[29,30] To calculate silver chloro complex production, we used the Ag concentrations detected as soluble silver in 1×, 5×, 10×, 15×, 20×, or 30× ERM (Fig. 3e).

Toxicity testing of SNCs or $AgNO_3$ at different ERM salinities

SNCs at concentrations as high as 18 mg/L were not lethal to the medaka eggs in 1× ERM, and all of the exposed eggs hatched (Fig. S2). Therefore, 15 medaka eggs (stage 21) in triplicate were exposed to 5 mL of SNCs (10 mg/L) or $AgNO_3$ (15.7 mg/L, as 10 mg/L silver) in each concentration of ERM (1×, 5×, 10×, 15×, 20×, or 30×) at pH 7 and 25 ºC in the dark until hatching or for 14 days. There were no significant differences in dissolved oxygen concentration (8.30 ± 0.04 mg/L) among the ERM solutions. The test solutions were renewed once a day. On day 6 of exposure, heart rate per 15 s was counted and eye size (diameter) was measured. The hatch rate was counted for 14 days. Full body lengths of post-hatch larvae were measured on hatching day under a dissecting microscope (SZ-ET, Olympus Co., Tokyo, Japan) with a micrometer. Medaka eggs in 1× to 30× ERM at pH 7 were used as controls.

Measurement of diameter of aggregated SNCs in ERM solutions

To investigate how ERM solutions of different salinity affected the status of colloidal silver and how silver aggregates were formed, SNCs (20 mg/L) in triplicate were added to each concentration of ERM (pH 7; 1×, 2.5×, 5×, 10×, 15×, or 30×) to a final concentration of 10 mg/L; the mixture was then stirred for 24 h at 25 ºC in the dark. The mixtures were subjected to particle diameter measurement with a Zetasizer Nano ZS two-angle particle and molecular size analyser (Malvern Instruments Ltd, Malvern, Worcestershire, United Kingdom). Precipitates were observed under a dissecting microscope.

Measurement of osmotic pressure

Two hundred medaka eggs (stage 21) were incubated in each concentration of ERM (1×, 5×, 10×, 15×, 20×, or 30×) at pH 7 and 25 ºC in the dark for 24 h, and then osmotic pressures of their body fluids were measured. See Supplemental Information for details.

Measurement of electrical resistance

To examine salinity-dependent ion permeation, we measured the electrical resistance of the egg chorion in each concentration of ERM (1×, 5×, 10×, 15×, 20×, or 30×) at pH 7 and 25 ºC. See Supplemental Information for details.

Measurement of silver uptake by medaka embryos and soluble silver

To investigate the effects of osmotic pressure on silver uptake through the chorion, 15 medaka eggs (stage 21) in triplicate were exposed to SNCs (10 mg/L) or $AgNO_3$ (15.7 mg/L, as 10 mg/L silver) in each concentration of ERM (1×, 5×, 10×, 15×, 20×, or 30×) at pH 7 and 25 ºC in the dark for 5 days (before hatching). The test solutions were renewed once a day. After exposure (on day 6), the eggs were washed with fresh and clean ERM at the respective concentrations (5 mL, 5 times). The embryos were then dechorionated with medaka hatching enzyme. Finally, the dechorionated embryos were washed with fresh and clean ERM at the respective concentrations (5 mL, 5 times). The amount of silver that accumulated in the dechorionated embryos was analysed by using inductively coupled plasma mass spectrometry (ICP-MS). To calculate the silver concentrations in the embryos, the fresh weight of a single embryo was measured with an analytical balance (MS204S, Mettler Toledo International Inc., Griefensee, Switzerland) to be 0.658 ± 0.027 mg. Test solutions (50 µL) were filtered through a 3-kDa membrane filter to obtain soluble silver; the concentration of soluble silver was then analysed by using ICP-MS. See Supplemental Information for details.

Statistical analyses

Data were analysed by using analysis of variance (ANOVA, $P < 0.05$) and Dunnett's *a posteriori* test to evaluate the impact of silver compared with references.

Results and discussion

Characterization of SNC and $AgNO_3$ solutions at different ERM concentrations

To characterize the SNCs, we measured their aggregated size and investigated the forms of soluble silver present, including silver chloro complexes.

SNCs aggregated with increasing salinity; we measured their diameters in ERMs of different salinities. The diameter of colloidal silver was 28.4 ± 8.5 nm in distilled water; the diameter was 67.8 ± 19.4 nm in 1× ERM (which has an osmotic pressure equivalent to that of freshwater) and 437.3 ± 71.6 nm in 30× ERM (which has an osmotic pressure equivalent to that of seawater). In higher concentrations of ERM (2.5×, 5×, 10×, 15×, or 30×) the measured diameters were larger than those in distilled water or 1× ERM and ranged between 352.8 and 504.5 nm. Between 2.5× ERM and 30× ERM, the average diameter was 435.2 ± 62.5 nm. There were no significant differences among the diameters at these salinities (Fig. S3).

Generally, when silver is added to saline solutions, soluble silver complexes such as silver chloro complexes ($[AgCl]^0$, $[AgCl_2]^-$, $[AgCl_3]^{2-}$ and $[AgCl_4]^{3-}$) are produced.[29,30] These complexes each have their own absorption spectra.[29] SNC or $AgNO_3$ solutions were scanned with a UV-Vis-NIR spectrophotometer (Fig. 1a and 1b, respectively) and different scan data were obtained in the UV-Vis range. In ultrapure water, the maximum absorption wavelengths of the SNC (396 nm) and $AgNO_3$ (198 nm) solutions differed markedly (Figs 1a and 1b). The peak absorbance at 396 nm, representing the presence of SNCs dispersed as colloids, was almost the same as the 390 nm reported by Liu and Hurt[31] for silver nanoparticles (diameter, 1.9 nm). In filtered or unfiltered 30× ERM solution the peak at 396 nm disappeared; instead, a peak at *ca*. 220 nm representing soluble silver emerged in both SNC solutions (Fig. 1a). The scan data for these filtered and unfiltered SNC solutions were almost the same. This was because in the unfiltered solution of SNCs in 30× ERM, portions of the SNCs were aggregated and were precipitated out (Fig. S4). Although a whole, unfiltered solution of SNCs in 30× ERM was subjected to scanning, it consisted largely of supernatant, whereas in the equivalent filtered solution, the aggregated SNCs, including precipitates, were filtered out. Precipitation was not observed in $AgNO_3$ in 30× ERM solution.

In ultrapure water, the maximum absorption wavelength of $AgNO_3$ solution (198 nm) was almost the same as the secondary

Cite this: DOI: 10.1039/c0xx00000x

www.rsc.org/xxxxxx

ARTICLE TYPE

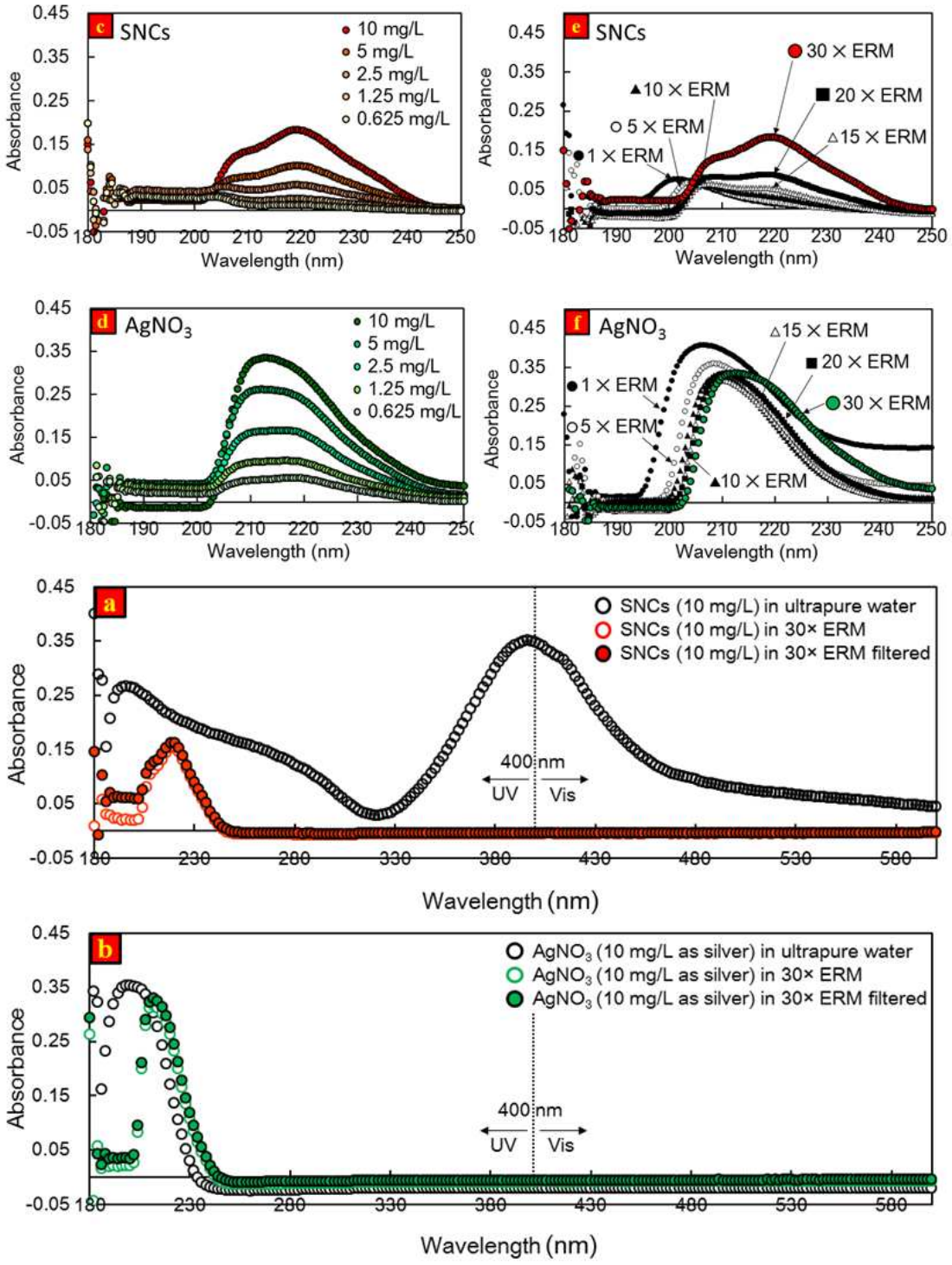

Fig. 1 Wavelength scanning of silver nanocolloids (SNCs) and silver nitrate solutions. (a) SNCs (10 mg/L) in ultrapure water or 30× ERM (filtered and unfiltered). (b) Silver nitrate (10 mg/L as silver) in ultrapure water or 30× ERM (filtered and unfiltered). (c) SNCs (0.625 to 10 mg/L) in 30× ERM. (d) Silver nitrate (0.625 to 10 mg/L) in 30× ERM. (e) SNCs (10 mg/L) in 1× to 30× ERM. (f) Silver nitrate (10 mg/L as silver) in 1× to 30× ERM. Blank data (ultrapure water or each ERM) have been subtracted from all data shown.

Cite this: DOI: 10.1039/c0xx00000x

www.rsc.org/xxxxxx

ARTICLE TYPE

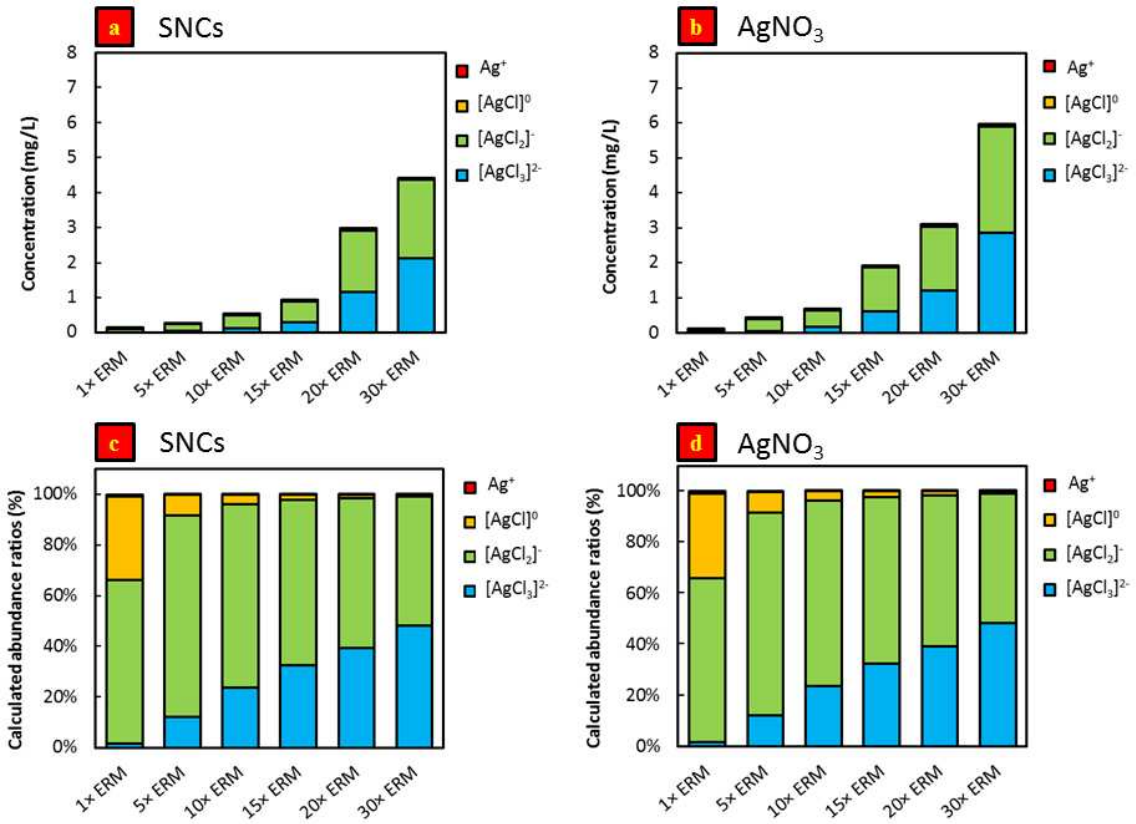

Fig. 2 Calculated concentration and abundance ratios of silver ions and silver chloro complex species. Concentration of silver ions and silver chloro complex species in different concentrations of ERM were calculated by using Visual MINTEQ version 3.0. (a) Concentrations of silver ion and silver chloro complex species in SNC solution. (b) Concentrations of silver ion and silver chloro complex species in silver nitrate ($AgNO_3$) solution. (c) Abundance ratios of silver ions and silver chloro complex species in SNC solution. (d) Abundance ratios of silver ions and silver chloro complex species in $AgNO_3$ solution.

peak for SNCs in ultrapure water (196 nm) (Figs 1a and 1b). The scan data for the filtered and unfiltered $AgNO_3$ solutions were almost the same, because in both cases the $AgNO_3$ was ionized and formed silver chloro complexes in solution.

Thus, with SNCs there was a peak at 396 nm in ultrapure water. In contrast, although the absorption spectra of soluble silver from SNCs and $AgNO_3$ in the 30× ERM solutions differed slightly, soluble silver had a peak at about 210 to 220 nm in all of the 30× ERM solutions (Figs 1a and 1b). This meant that the UV-Vis-NIR spectrophotometer detected both SNCs and soluble silvers. In this case, aggregated SNCs were precipitated and were thus not detected by the UV-Vis-NIR spectrophotometer.

Production of soluble silver chloro complexes ($[AgCl]^0$, $[AgCl_2]^-$, $[AgCl_3]^{2-}$, and $[AgCl_4]^{3-}$) depends on the chloride concentration.[29,30] To determine the differences in complex formation between the SNC and $AgNO_3$ solutions, we obtained scan data at different silver or ERM concentrations.

In solutions that had different silver concentrations but were fixed at 30× ERM, although peaks at 219 nm (SNCs) and 213 nm ($AgNO_3$) emerged, the patterns of the absorption spectra of all SNC solutions were similar; this was also true for all of the $AgNO_3$ solutions (Figs 1c and 1d).

In solutions that had different ERM concentrations but were fixed at 10 mg/L silver concentration, the patterns of the absorption spectra of SNCs differed among different ERM solutions: the peak shifted gradually from 201 nm at 1× ERM to 208 and 219 nm at 30× ERM. The patterns of the absorption spectra of $AgNO_3$ did not differ among the different ERM solutions, although the peak shifted gradually from 207 nm at 1× ERM to 213 nm at 30× ERM (Figs 1e and 1f).

To examine the salinity-dependent production of soluble silver chloro complexes from SNCs or $AgNO_3$, we measured the concentrations of soluble silver in filtered SNC or $AgNO_3$ solutions. Although the initial concentrations in the two types of solution were the same at 10 mg/L, the soluble silver concentrations detected increased with increasing ERM concentration (Fig. 3e). The complex species included in each solution would have differed among salinities, because the patterns of the absorption spectra differed markedly (Figs 1e and 1f).

By using the concentrations of Ag detected as soluble silver in 1×, 5×, 10×, 15×, 20×, and 30× ERM (Fig. 3e), we calculated the theoretical concentrations of silver chloro complexes (Figs 2a and 2b). Major silver chloro complexes were $[AgCl]^0$, $[AgCl_2]^-$, and $[AgCl_3]^{2-}$ in both the SNC solution and the $AgNO_3$ solution (Figs 2c and 2d). These accounted for more than 99% of the soluble silvers. Ag^+ accounted for less than 1% of the soluble silvers (Tables S1 and S2). This calculation was based on the hypothesis that existing soluble silver would react with anions, including Cl^-, OH^-, HCO_3^-, and SO_4^{2-} (all of which were derived from the ERM), or with NO_3^- (which was derived from the $AgNO_3$), in each solution. Although there were marked differences between the patterns of the absorption spectra of SNCs and $AgNO_3$ (Figs 1e and 1f), the two sets of complex-formation data simulated by the software program were almost the same and could not explain the different patterns of the absorption spectra (Figs 2a to 2d and Tables S1 and S2). In theory, $[AgCl_4]^{3-}$ must have been produced[29,30]; however, the software program does not support $[AgCl_4]^{3-}$. Moreover, insoluble AgCl is not supported; however, precipitates were formed in the SNC solution (Fig. S4) but not in the $AgNO_3$ solution. When stepwise formation constants were used for Cl^- and Ag^+, $[AgCl_4]^{3-}$ was the dominant chloro complex, followed by $[AgCl]^0$, $[AgCl_2]^-$, and $[AgCl_3]^{2-}$ (Figs S5a and S5b and Table S3). Regardless, both types of calculations indicate that at least $[AgCl]^0$, $[AgCl_2]^-$, and $[AgCl_3]^{2-}$ must be major complexes and may be involved in the toxic effects of SNCs.

Although the patterns of the absorption spectra of SNCs and $AgNO_3$ differed markedly and precipitates formed only in the SNC solution, the simulation results for soluble silvers could not explain that the different patterns of absorption spectra and the precipitation. The difference is probably related to the physicochemical effects of SNC, but currently we have no clues as to its cause.

Toxic effects of SNCs at 1× ERM (freshwater conditions)

No hatching inhibition, malformation or mortality was observed in any of the medaka eggs exposed to SNCs at 1 to 18 mg/L in 1× ERM. The rates of hatching (Fig. S2), malformation, and mortality (data not shown) were almost 100%, 0.0%, and 0.0%, respectively, at all SNC concentrations. However, in ultrapure water, which has very low ionic strength, the presence of SNCs led to higher mortality rates than in 1× ERM; the 50% lethal concentration in 96 h (96-h LC_{50}) was 0.051 (0.0386 to 0.0703, 95% confidence limits) mg/L (data not shown). Park *et al.*[32] reported a similar toxic decline: the toxicity of citrate-capped silver nanoparticles was higher in water of low ionic strength than in water of high ionic strength. Groh *et al.*[33] summarised the effects of chloride concentration on the toxicity of silver nanoparticles to fish; they concluded that "high chloride concentrations in the exposure medium pose the risk of underestimating the LC_{50} values for silver nanoparticles." These alterations in silver toxicity are thus associated with changes in the ionic strength of the test solution. In ultrapure water, silver can exist as free Ag^+ and exhibit toxicity; however, in some ionic solutions such as freshwater, free Ag^+ combines with Cl^- to form insoluble AgCl;[29, 30] toxicity thus declines.

Salinity-dependent silver toxicity (freshwater to seawater conditions)

Medaka eggs were exposed to SNCs or to $AgNO_3$ at 10 mg/L (as silver) at different salinities. We then measured phenotypic biomarkers, namely hatching rate, full body length of post-hatch larvae, heart rate per 15 s, and eye size. In the controls, all embryos hatched at salinities ranging from 1× to 30× ERM; however, the hatching rate of SNC-exposed embryos decreased to 71% in 20× ERM (ANOVA, $P < 0.01$) compared with that in SNC-exposed embryos at 1× ERM, and only 2% of embryos hatched in 30× ERM (Fig. 3a). $AgNO_3$ did not significantly inhibit hatching by 20× ERM; it completely inhibited hatching only in 30× ERM compared with $AgNO_3$-exposed embryos at 1× ERM ($P < 0.01$). Full body length in the post-hatch larvae was consistently 4.55 to 4.69 mm at all ERM concentrations in the controls. With SNC exposure, although in 1× to 15× ERM the body length was in a similar range (4.33 to 4.59 mm) as in the controls, the average length decreased significantly to 3.77 in 20× ERM compared with that of SNC-exposed embryos at 1× ERM; moreover, it decreased to 3.75 mm in 30× ERM (statistical comparison was not performed at this concentration because of an insufficiency of samples) (Fig. 3b). $AgNO_3$ exposure caused no significant difference in full body length compared with that in 1× ERM. Heart rate per 15 s in the controls was not constant and ranged from 29.6 to 32.2 throughout the range from 1× to 30× ERM. Although the heart rate was not very stable in the controls, or with SNC or $AgNO_3$ exposure, with SNC or $AgNO_3$ exposure the heart rate was significantly ($P < 0.01$) lower in both types of solution at 30× ERM than at 1× ERM (Fig. 3c). Eye size was stable at 0.357 to 0.366 mm at all ERM concentrations in the controls. In 1× to 15× ERM, eye size was in a similar range (0.344 to 0.357 mm) with SNC or $AgNO_3$ exposure as in the controls; however, in 20× ERM and 30× ERM it was significantly lower ($P < 0.01$) with SNC or $AgNO_3$ exposure than in 1× ERM (Fig. 3d).

Groh *et al.*[33] stated that chloride reduces the toxicity of silver nanoparticles. However, the salinities they examined were lower than 1× ERM. In our research, SNC toxicity was higher in ultrapure water than in 1× ERM. Under freshwater conditions, free Ag^+ is no longer dominant; soluble complexes ($[AgCl]^0$ and $[AgCl_2]^-$) are formed and dominate (Figs 2a to 2d, Figs S5a and S5b, and Table S1 to S3). These complexes seem to be less toxic than free Ag^+. In 1× to 30×ERM, $[AgCl_3]^{2-}$ or $[AgCl_4]^{3-}$, or both, emerged and dominated along with $[AgCl_2]^-$ (Figs 2a to 2d, and Figs S5a and 5b). Simultaneously, the exposed medaka embryos exhibited toxic effects (Figs 3a to 3d). $[AgCl_3]^{2-}$ or $[AgCl_4]^{3-}$—or both—seem to have toxicity.

Thus, although the concentration of SNCs or $AgNO_3$ in all test solutions was 10 mg/L (as silver), these four biomarkers were affected by an increase in salinity. Notably, hatching rate was the most sensitive to SNC toxicity, and the toxicity of SNCs to hatching was greater than that of $AgNO_3$.

To measure the concentrations of soluble silver complexes, we analysed filtered solutions of SNCs or $AgNO_3$ at 10 mg/L (as silver) with ICP-MS (Fig. 3e). The concentration of soluble silver increased from 0.08 mg/L (SNCs) and 0.06 mg/L ($AgNO_3$) in 1×ERM to 2.45 mg/L (SNCs) and 3.30 mg/L ($AgNO_3$) in 30× ERM. In 20× ERM, although the soluble silver concentrations in the SNC and $AgNO_3$ solutions were the same, the hatching rate was significantly ($P < 0.01$) inhibited in the SNC solution but not

Cite this: DOI: 10.1039/c0xx00000x

www.rsc.org/xxxxxx

ARTICLE TYPE

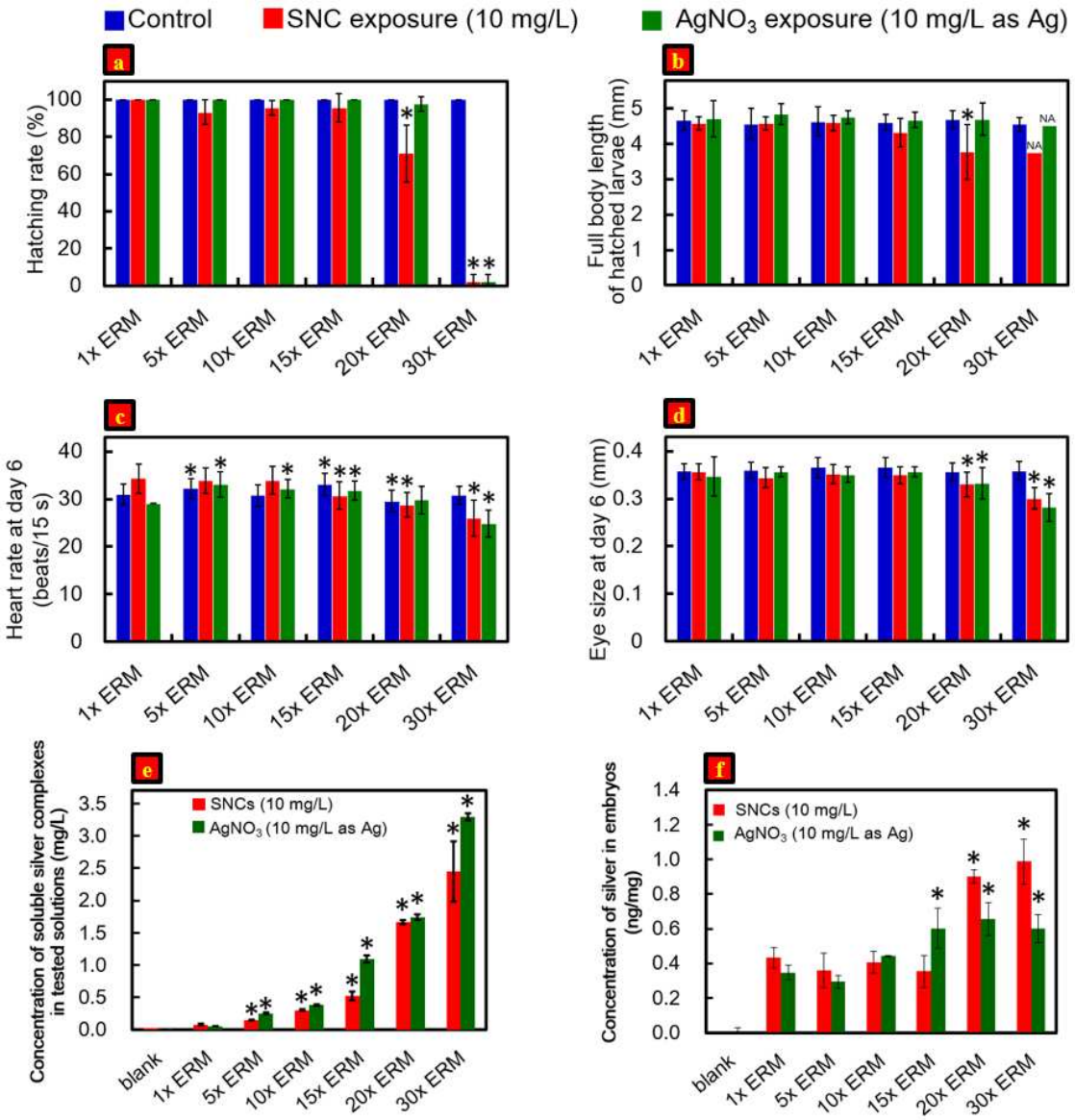

Fig. 3 Measured phenotypic biomarkers and uptake of silver in medaka eggs exposed to silver nanocolloids (SNCs) or silver nitrate. Medaka eggs at stage 21 were exposed to SNCs (10 mg/L) or silver nitrate (10 mg/L as silver) in different concentrations of ERM for 6 days. (a) Hatching rate. (b) Full body length. (c) Heart rate per 15 s. (d) Eye size. (e) Concentrations of soluble silver complexes released from SNCs or silver nitrate into test solutions. (f) Silver concentrations in embryos exposed to SNCs or silver nitrate in different concentrations of ERM. *Significant difference compared with the respective 1× ERM solution. NA: not available because only one larva hatched.

in the $AgNO_3$ solution (compare Figs 3a and 3e).

The accumulated silver concentrations in the embryos were 0.43 ± 0.060 ng/mg (SNCs, 1× ERM) and 0.35 ± 0.042 ng/mg ($AgNO_3$, 1× ERM); these increased to 0.99 ng/mg (SNCs, 30× ERM) and 0.60 ng/mg ($AgNO_3$, 30× ERM) with the increase in salinity. In our previous study[7] using other silver nanocolloids (3.6 nm in diameter, with a 96-h LC_{50} of 1.39 ± 0.02 mg/L in ultrapure water) made by a different company, silver was detected at levels of 0.025 ng/mg in medaka embryos exposed to 0.5 mg/L in ultrapure water. In our present study, medaka eggs were exposed to silver at 10 mg/L— a concentration 20 times the 0.5 mg/L. Generally higher concentrations in ambient water cause higher bioaccumulations in aquatic organisms. This is why greater accumulation of silver occurred in our present study. Measurement of the concentrations of silver in the embryos revealed that significantly more silver accumulated with SNC exposure than with $AgNO_3$ exposure in 20× and 30× ERM ($P < 0.01$) (Fig. 3f). The greater toxicity with SNCs than with $AgNO_3$

at 20× ERM (Figs 3a and 3b) probably occurred because the bioavailability of silver through the egg chorion was significantly higher with SNCs than with $AgNO_3$ in 20× or 30× ERM ($P < 0.01$).

Osmotic pressures in medaka egg embryos, and bioavailability of SNCs

Salinity-dependent membrane permeation of chemicals has been reported in the cases of mercury chloride,[20] contaminant chemicals at waste-disposal landfill sites,[21] and nanoparticles.[22] To investigate salinity-dependent increases in the bioavailability of silver, we measured the electrical resistance of the chorion membrane in each concentration of ERM (1×, 5×, 10×, 15×, 20×, or 30×) (Fig. S6 and Formula S1). Although the mean egg diameter was 1.29 ± 0.02 mm at all ERM concentrations and did not change during incubation at any of the concentrations (Table S4), the electrical resistance of the chorion membrane decreased with increasing salinity (i.e. with increasing ERM concentration from 1× to 30×) under a constant voltage (0.4 V) (Fig. 4a). This trend was the same at higher voltages measured up to 2.0 V (Fig. 4b). Thus, there was salinity-dependent ion permeation between the chorion and the ERM. Hence, the increasing accumulation of SNCs or soluble silver chloro complexes, or both, by embryos *via* the chorion membrane can be explained by increasing osmotic pressure of ERM and decreasing resistance.

In addition, incubation of the eggs in ERM at different concentrations for 24 h revealed that the osmotic pressure of embryonic fluids increased with increasing ERM concentration, as Machado and Podrabsky[34] reported (Fig. S7a). There was a linear relationship ($r = 0.9754$, $P < 0.01$) between the osmotic pressure of the embryonic fluids and the osmotic pressure (and by implication the salinity) of the incubation solution (Fig. S7b).

In our previous study, water–suspended fluorescent nanoparticles were demonstrated to penetrate through the medaka egg chorion in 1× ERM; particles 474 nm in diameter showed the greatest uptake into the egg. Furthermore, uptake of nanoparticles increased with increasing salinity.[22] In this study, we estimated the aggregated diameter of SNCs in 30× ERM to be 437.3 nm (Fig. S3)—close to the size that shows the greatest uptake. Moreover, a study of the toxicity of contaminant chemicals at waste-disposal landfill sites found that medaka embryonic malformation was induced most frequently when there was osmotic equivalency of leachate to eggs.[21] These findings support the salinity dependence of the increase in silver bioavailability in the embryos.

Conclusion

We demonstrated here that increasing salinity facilitates the uptake of ion-charged compounds such as SNCs and silver chloro complexes into medaka eggs via the cholion. Salinity affects the electrical resistance of the chorion membrane and the embryonic osmotic pressure; these in turn affect the permeation of ion–charged chemicals through the chorion. Not only are potentially toxic silver chloro complexes released, but also the bioavailability of SNCs is higher than that of $AgNO_3$ in saline solutions, meaning that SNCs have greater medaka embryo toxicity. Although we do not yet know precisely which SNC-related compounds have toxic effects, silver nanotoxicity must be taken into consideration in high-salinity aquatic environments to a greater extent than in freshwater environments.

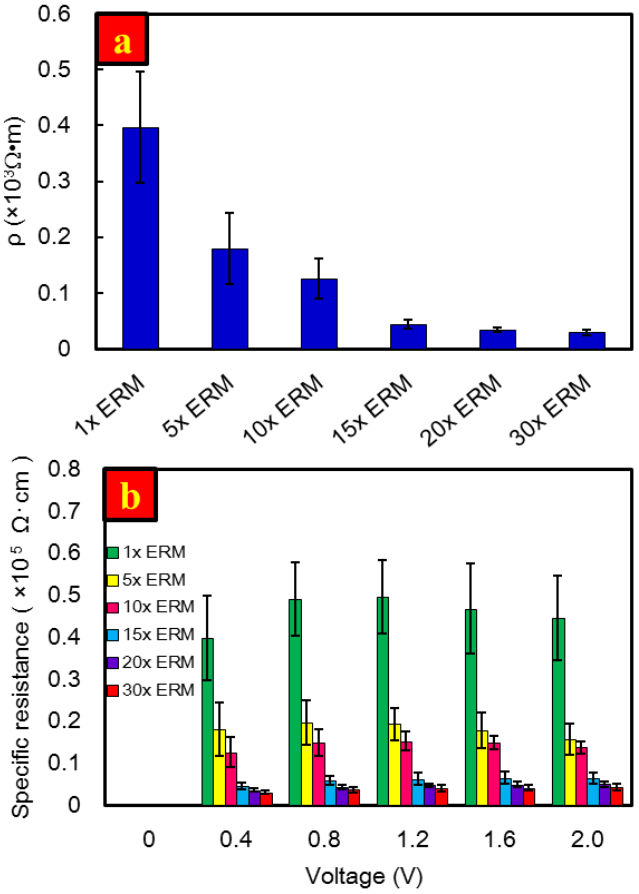

Fig. 4 Electrical resistance of medaka eggs in different concentrations of ERM (a) at a constant voltage of 0.4 V and (b) at voltages of 0.4 to 2.0 V.

Acknowledgments and grant information

We are grateful to Ms Kaori Shimizu and Mr Masaki Takasu of the Department of Life Sciences, Toyo University for their technical support. This project was supported by research grants from the Special Research Foundation and Bio-Nano Electronics Research Centre of Toyo University (to SK); by the Science Research Promotion Fund of the Promotion and Mutual Aid Corporation for Private Schools of Japan (to SK); by the New Project Fund for Risk Assessments, from the Ministry of Economy, Trade and Industry (to SK); by a Grant-in-Aid for Challenging Exploratory Research (award 23651028 to SK); by a Grant-in-Aid for Scientific Research (B) (award 23310026-0001 to SK); and by a Grant-in-Aid for Strategic Research Base Project for Private Universities (award S1411016 to SK), from the Ministry of Education, Culture, Sports, Science and Technology of Japan.

Notes

[a] *Graduate School of Life Sciences, Toyo University, 1-1-1 Izumino, Itakura, Gunma 374-0193, Japan.*
[b] *Research Centre for Life and Environmental Sciences, Toyo University, 1-1-1 Izumino, Itakura, Gunma 374-0193, Japan.*

*Corresponding author. Tel: 81-276-82-9029; fax: 81-276-82-9029; e-mail: kashiwada@toyo.jp.

† Electronic Supplementary Information available: [details of any supplementary information available should be included here]. See DOI:10.1039/b000000x/

‡*Safety:* The Japanese medaka used were treated humanely in accordance with the institutional guidelines of Toyo University, with due consideration for the alleviation of distress and discomfort.

References

1 A. Nel, T. Xia, L. Madler and N. Li, Toxic potential of materials at the nanolevel. *Science*, 2006, **311**, 622–627.

2 Cientifica Nanotubes 2004 (Excecutive Summary available at http://www.cientifica.eu).

3 P. Asharani, Y. Wu, Z. Gong and S. Valiyaveettil, Toxicity of silver nanoparticles in zebrafish models. *Nanotechnology*, 2008, **19**, 255102.

4 O. Bar-Ilan, R. M. Albrecht, V. E. Fako and D. Y. Furgeson, Toxicity Assessments of Multisized Gold and Silver Nanoparticles in Zebrafish Embryos. *Small*, 2009, **5**, 1897–1910.

5 M. K. Yeo and M. Kang, Effects of nanometer sized silver materials on biological toxicity during zebrafish embryogenesis. *Bulletin of the Korean Chemical Society*, 2008, **29**, 1179–1184.

6 K. M. Newton, H. L. Puppala, C. L. Kitchens, V. L. Colvin, and J. Klaine, Silver nanoparticle toxicity to daphnia magna is a function of dissolved silver concentration. *Environmental Toxicology and Chemistry*, 2013, **32**, 1–9

7 S. Kashiwada, M. E. Ariza, T. Kawaguchi, Y. Nakagame, B. S. Jayasinghe, K. Gärtner, H. Nakamura, Y. Kagami, T. Sabo-Attwood, P. L. Ferguson and G. T. Chandler, Silver Nanocolloids Disrupt Medaka Embryogenesis through Vital Gene Expressions. *Environmental Science & Technology*, 2012, **46**, 6278–6287.

8 A. Bianchini, R. C. Playle, C. M. Wood and P. J. Walsh, Mechanism of acute silver toxicity in marine invertebrates. *Aquatic Toxicology*, 2005, **72**, 67–82.

9 B. K. Gaiser, A. Biswas, P. Rosenkranz, M. A. Jepson, J. R. Lead, V. Stone, C. R. Tyler and T. F. Fernandes, Effects of silver and cerium dioxide micro- and nano-sized particles on Daphnia magna. *Journal of Environmental Monitoring*, 2011, **13**, 1227–1235.

10 E. Navarro, F. Piccapietra, B. Wagner, F. Marconi, R. Kaegi, N. Odzak, L. Sigg and R. Behra, Toxicity of silver nanoparticles to Chlamydomonas reinhardtii. *Environ Sci Technol*, 2008, **42**, 8959–8964.

11 L. Šiller, M.-L. Lemloh, S. Piticharoenphun, B. G. Mendis, B. R. Horrocks, F. Brümmer and D. Medaković, Silver nanoparticle toxicity in sea urchin Paracentrotus lividus. *Environmental Pollution*, 2013, **178**, 498–502.

12 R. Suwa, C. Kataoka, S. Kashiwada, Effects of silver nanocolloids on early life stages of the scleractinian coral *Acropora japonica*, Marine Environmental Research, 2014, **99**, 198–203

13 S. A. Villalobos, J. T. Hamm, S. J. Teh and D. E. Hinton, Thiobencarb-induced embryo toxicity in medaka (Oryzias latipes): stage-specific toxicity and the protective role of chorion. *Aquatic Toxicology*, 2000, **48**, 309–326.

14 R. Behra, L. Sigg, M. J. D. Clift, F. Herzog, M. Minghetti, B. Johnston, A. Petri-Fink and B. Rothen-Rutishauser, Bioavailability of silver nanoparticles and ions: from a chemical and biochemical perspective. *Journal of The Royal Society Interface*, 2013, 10.

15 J. Fabrega, S. N. Luoma, C. R. Tyler, T. S. Galloway and J. R. Lead, Silver nanoparticles: Behaviour and effects in the aquatic environment. *Environment International*, 2011, **37**, 517–531.

16 Y. Hayashi, T. Miclaus, C. Scavenius, K. Kwiatkowska, A. Sobota, P. Engelmann, J. J. Scott-Fordsmand, J. J. Enghild and D. S. Sutherland, Species differences take shape at nanoparticles: protein corona made of the native repertoire assists cellular interaction. *Environmental Science & Technology*, 2013, **47**, 14367–14375.

17 R. J. Griffitt, K. Hyndman, N. D. Denslow, D. S. Barber, Comparison of molecular amd histological changes in zebrafish gills exposed to metallic nanoparticles, Toxicological science, 2009, 107(2), 404–415

18 Y. Yue, R, Behra, L. Sigg, P. F. Freire, S. Pillai, K. Schirmer, Toxicity of silver nanoparticles to a fish gill cell line: Role of medium composition, *Nanotoxicology*, 2014, **12**, 1–10

19 T. Iwamatsu, Stage of normal development in medaka *Oryzias latipes*, *Mechanisms of Development*, 2004, **121**, 605–618

20 M. Sakaizumi, Effect of inorganic salts on mercury-compound toxicity to the embryos of the medaka (Oryzias latipes). *J Faculty Sci, Univ Tokyo, Sec IV*, 1980, **14**, 369–384.

21 K. Sumitani, S. Kashiwada, K. Osaki, M. Yamada, S. Mohri, S. Yasumasu, I. Iuchi and Y. Ono, Medaka (Oryzias latipes) Embryo toxicity of treated leachate from waste-landfill sites. *J Jpn Society of Waste Manage Exp*, 2004, **15**, 472–479.

22 S. Kashiwada, Distribution of nanoparticles in the see-through medaka (Oryzias latipes). *Environ Health Perspect*, 2006, **114**, 1697–1702.

23 A. Hirai, Fine Structure of the Egg Membranes in Four Species of Pleuronectinae. *Japanese Journal of Ichthyology*, 1993, 40, 227–235.

24 A. J. Van Wettere, J. M. Law, D. E. Hinton and S. W. Kullman, Anchoring hepatic gene expression with development of fibrosis and neoplasia in a toxicant-induced fish model of liver injury. *Toxicologic Pathology*, 2013, **41**, 744–760.

25 S. Kashiwada, H. Tatsuta, M. Kameshiro, Y. Sugaya, T. Sabo-Attwood, G. T. Chandler, P. L. Ferguson and K. Goka, Stage-dependent differences in effects of carbaryl on population growth rate in Japanese medaka (Oryzias latipes). *Environmental Toxicology and Chemistry*, 2008, **27**, 2397–2402.

26 T. Iwamatsu, *The Integrated Book for the Biology of the Medaka*, University Education Press, Japan, 1997.

27 T. Miyamoto, T. Machida and S. Kawashima, Influence of environmental salinity on the development of chloride cells of freshwater and brackish-water medaka,Oryzias latipes. *Zoological Science*, 1986, **3**, p859–865.

28 K. Inoue and Y. Takei, Diverse Adaptability in Oryzias Species to High Environmental Salinity. *Zoological science*, 2002, **19**, 727–734.

29 A. Ringbom, *Complexation in analytical chemistry: a guide for the critical selection of analytical methods based on complexation reactions*, Interscience Publishers, 1963.

30 R. Eisler, Silver hazards to fish, wildlife, and invertebrates: a synoptic review, U. S. Department of the interior national biological service Patuxent wildlife research center, 1996

31 J. Liu and R. H. Hurt, Ion Release Kinetics and Particle Persistence in Aqueous Nano-Silver Colloids. *Environmental Science & Technology*, 2010, **44**, 2169–2175.

32 K. Park, G. Tuttle, F. Sinche, S. L. Harper, Stability of citrate-capped silver nanoparticles in exposure media and their effects on the development of embryonic zebrafish (*Danio rerio*). *Arch. Pharm. Res*, 2013, **36**, 125–133

33 K. J. Groh, T. Dalkvist, F. Piccapietra, R. Behra, M. J. Suter, K. Schirmer, Critical influence of chloride ions on silver ion-mediated acute toxicity of silver nanoparticles to zebrafish embryos, *Nanotoxicology*, 2014, **14**, 1–11

34 B. E. Machado and J. E. Podrabsky, Salinity tolerance in diapausing embryos of the annual killifish Austrofundulus limnaeus is supported by exceptionally low water and ion permeability. *Journal of Comparative Physiology B-Biochemical Systemic and Environmental Physiology*, 2007, **177**, 809–820.

Table of contents